Dynamics of Complex Truss-Type Space Structures

Y. Yong* and Y. K. Lin† Florida Atlantic University, Boca Raton, Florida

A mathematical procedure is presented for the analysis of the dynamical behavior of truss-type space structures composed of spatially periodic truss units, or sections of spatially periodic units. These units are connected end-to-end to form an array, or intersecting arrays. Attention is focused on the steady-state response of such a structure to a sinusoidal excitation, and on the transient response to an impulsive excitation. The two types of responses are related essentially as a Fourier transform pair. The steady-state response to a sinusoidal input is treated as superposition of wave motions, taking into account the effects of wave reflection due to the change in the construction pattern along the structure, intersections, and boundary conditions. Since damping usually exists in a real structure, a wave motion decays as it propagates along the structure. However, this can cause numerical difficulty in the analysis if the structure is sufficiently long, because a decaying wave appears as a growing wave in the opposite direction. Since propagations in both directions must be accounted for, computational errors associated with the apparent growing waves also grow, and the numerical results become meaningless. In the new scheme, use is made of the wave reflection and transmission matrices, making it possible for all computations to proceed in the direction of wave propagation, so that the results are always numerically stable, and for such complicated configurations as intersecting arrays to be treated quite simply. Application of the procedure is illustrated by an example.

 μ_o

Nomenclature

= clamped boundary at the right end

 C_r

w(j)

 w_{inn}

[D(n)]	= eigenvector matrix of the transfer matrix for cell n
F_{l}	= free boundary at the left end
$f(n_r)$	= force vector at the right end of cell n
f_{ext}	= vector of excitation forces at a core cell
f_s	= input force vector
[G]	= wave generation matrix
[K]	= stiffness matrix
[M]	= consistent mass matrix
$M_r(n)$	= submatrix of $[D(n)]$ converting right-going waves
	into a displacement vector
$N_l(n)$	= submatrix of $[D(n)]$ converting left-going waves
	into a force vector
n_r	= the right end of cell n
[Q(k,j)]	= wave-vector transfer matrix from j to k
Q_{pq}	= submatrices of $[Q(k,j)]$
R'(k,j)	= reflection matrix for the segment between j and k
	responding to right-going waves at j
$R^{l}(k,j)$	= reflection matrix for the segment between j and k
	responding to left-going waves at k
[S]	= wave scattering matrix
[T(k,j)]	= transfer matrix for state vector from j to k
$T^r(k,j)$	= transmission matrix for the segment between j and
	k responding to right-going waves at j
$T^l(k,j)$	= transmission matrix for the segment between j and
	k responding to left-going waves at k
/ • N	11 1

= vector of displacement at a core cell

= displacement vector at j

= input displacement vector

[Z]= impedance matrix = submatrices of [Z] Z_{ij} = circular frequency = diagonal matrix of eigenvalues of [T(k,j)] with ٨ magnitude smaller than one $\mu_r(n_r)$ = right-going wave vector at n_r = left-going wave vector at n_r $\mu_l(n_r)$ = incoming wave vector μ_i = outgoing wave vector

Introduction

UE to the requirements for light weight and high rigidity, truss-type construction has been the dominant form for proposed large space structures. Typically, such a structure is composed of several sections. Each section is composed of identical units that are connected end-to-end to form a spatially periodic array. Different sections may again be interconnected or intersect one another. The variety of possible configurations makes the analysis of large space structures difficult. In order to simplify the problem, rather sweeping approximations have been suggested (e.g., Refs. 1 and 2), in which the built-up truss-type structure is replaced by Timoshenko beam elements, or other continuum elements. The errors involved in such gross approximations can be quite significant. However, neither is an all-encompassing finite-element modeling a good approach, because the natural frequencies of a structure composed of periodic units are known to group closely in distinctive frequency bands, and the determination of closely valued natural frequencies and associated mode shapes can be both expensive and inaccurate.

In this paper, a mathematical procedure recently developed for the analysis of damped periodic and piece-wise periodic structures³ is extended to include the more complicated configurations of intersecting arrays. The procedure is a hybrid of finite element, transfer matrix, and wave propagation approaches, an idea proposed previously by von Flotow⁴ in dealing with structural networks of substituted continuum elements. The transfer matrix and wave propagation approaches have been applied separately and successfully for the analysis of periodic structures of much simpler configuration (e.g., Refs. 5-12), whereas a combination of finite element and transfer matrix formulation was first advocated by Mc-Daniel and Eversole.¹³ In the proposed hybrid procedure,

Received Feb. 6, 1989; presented as Paper 89-1307 at the AIAA/ ASME/ASCE/AHS 30th Structures, Structural Dynamics, and Materials Conference, Mobile, AL, April 3-5, 1989; revision received June 19, 1989. Copyright © 1990 American Institute of Aeronautics and Astronautics, Inc. All rights reserved.

^{*}Assistant Professor, Center for Applied Stochastics Research and Ocean Engineering Department. Member AIAA.

[†]Charles E. Schmidt Professor in Engineering, and Director, Center for Applied Stochastics Research. Associate Fellow AIAA.

finite-element formulation is used to model a periodic truss unit, or each type of periodic truss unit in the structure, so that the dynamic characters of such a unit can be represented as accurately as desired, regardless of its complexity. Traditional transfer matrices for state vectors are transformed to transfer matrices for wave vectors, ^{3,4} thus, various waves propagating along the structure in different directions can be identified and certain numerical difficulties can be circumvented. An example is given for illustration.

Truss Unit

A typical truss unit for a large space structure is shown in Fig. 1. The choice of the size of such a unit is arbitrary; thus, it can be judicially selected for the convenience of an analysis. In what follows, a truss unit will be referred to as a cell. It is assumed that the dynamical behavior of a cell has been determined adequately, using a finite-element approach. Thus, in our mathematical model, a cell can be regarded as the smallest component of the overall structure. Neighboring cells are assumed to be rigidly connected at a number of node points. In the case of Fig. 1, such nodes are the adjoining corners of neighboring cells. Each corner has six degrees of freedom, three in translation and three in rotation; thus, for the cell shown in Fig. 1, each end is capable of twenty-four generalized displacements. As will be explained later, this implies that a total of twenty-four wave motions can be transmitted through a cell.

Since we intend to develop a theory applicable to any type of cell unit, we shall consider a generic cell, labeled as cell n and shown in Fig. 2. The left end and the right end of the cell are denoted by n_l and n_r , respectively. Let p be the number of generalized displacements at each end, indicated by dotted lines in the figure.

It is usually simpler to formulate a dynamic response problem of a linear structure in terms of frequency response. In this case, the time dependence of the motion is sinusoidal. The transient response due to impulsive excitation can be obtained indirectly by Fourier transformation.

For simplicity, the frequency dependence in an expression for sinusoidal motion will not be indicated in the subsequent development unless there is a possibility of confusion. The generalized displacements and corresponding generalized forces at the ends of a cell are represented as two p-dimensional vectors w() and f(), respectively. Using a finite-element formulation, we can construct an impedance matrix [Z], such that

$$[Z] \begin{cases} w(n_l) \\ w(n_r) \end{cases} = \begin{cases} -f(n_l) \\ f(n_r) \end{cases} \tag{1}$$

where [Z] is given by

$$[Z] = -\omega^2[M] + [K]$$
 (2)

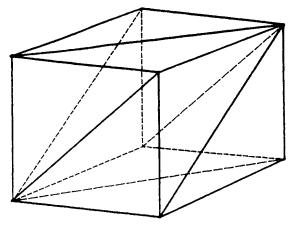


Fig. 1 A typical truss unit.

Fig. 2 A generic cell unit of periodic or piecewise periodic structure.

and where [M] is a consistent mass matrix, [K] is a stiffness matrix, and ω is frequency. The sign convention adopted for the force vectors follows what is usually used in a transfer matrix formulation, which accounts for the negative sign for $f(n_l)$ in Eq. (1). Comparing Eq. (1) with the following transfer matrix relation

it can be shown that

$$[T(n_{P}, n_{l})] = \begin{bmatrix} -Z_{12}^{-1} Z_{11} & -Z_{12}^{-1} \\ Z_{21} - Z_{22} Z_{12}^{-1} Z_{11} & -Z_{22} Z_{12}^{-1} \end{bmatrix}$$
(4)

where the transfer matrix [T] is $2p \times 2p$. The 2p-dimensional vector $\{w(n), f(n)\}$ at either end of a cell is referred to as a state vector. The construction of a transfer matrix from the corresponding impedance matrix is, of course, not new. It has been used, for example, in Refs. 13 and 14.

Now, consider a transformation

where [D] is $2p \times 2p$. Substituting the above into Eq. (1) yields

$$\mu(n_r) = [D(n)]^{-1} [T(n_r, n_l)] [D(n)] \ \mu(n_l) \tag{6}$$

If columns in [D(n)] are eigenvectors of $[T(n_r, n_l)]$, then

in which λ_j , j = 1, 2, ..., 2p, are the eigenvalues of matrix $[T(n_r, n_l)]$.

Now we shall make use of an important property common to all transfer matrices⁵; namely, for every eigenvalue λ_i , there exists a $\lambda_{p+i} = \lambda_i^{-1}$. Physically, each pair of reciprocal eigenvalues is associated with two wave motions of the same type, but propagating in two opposite directions. Thus, Eq. (6) can be rewritten as follows:

where

$$[\Lambda] = \begin{bmatrix} \lambda_1 & & \\ & \ddots & \\ & & \lambda_p \end{bmatrix}$$
 (9)

and where each μ will be referred to as a wave vector in what follows

Since damping generally exists in a real structure, the eigenvalues λ_i are complex-valued. For computational efficiency to be explained later, we arrange the eigenvalues such that their absolute values are in ascending order. Then it can be shown that $|\lambda_i| < 1$, where λ_i are the elements in the diagonal matrix Λ that appeared in Eq. (9). If the eigenvalues are so arranged,

then elements of μ_r and μ_l in Eq. (8) are, respectively, complex amplitudes of right-going and left-going wave motions. The absolute value of each λ_l accounts for the reduction in magnitude when the associated wave motion propagates across a cell, and its phase represents the difference in phase at the two locations n_r and n_l . Equation (8) shows that the amplitude of a wave motion always decreases when propagating across a cell. This is a result of energy dissipation, since no power is supplied within the cell.

For the convenience of the following discussion, we introduce submatrices $M_r(n)$, $M_l(n)$, $N_r(n)$, and $N_l(n)$ of [D]. These submatrices are of order $p \times p$, and their roles are revealed by rewriting Eq. (5), as follows:

It is clear that $M_r(n)$ and $M_l(n)$ combine the right-going and left-going waves into displacements $w(n_r)$, and that $N_r(n)$ and $N_l(n)$ combine these waves into forces $f(n_r)$.

We digress to comment on the precise meaning of wave motions in the above context. First, it should be noted that we are concerned only with the motions at the ends of a cell, namely at n_r and n_l . Detailed information within a cell remains unspecified. However, if we were to examine the motions within individual members which constitute the whole cell, we would find other types of waves. Since these individual members are usually thin uniform bars, we would find essentially damped sinusoidal waves in bending, torsion, shear, and longitudinal motions. At each joint where different members meet, complicated scattering would occur. Yet the resulting motion at the ends of each cell would have the relationship represented by Eq. (8). The advantage of restricting our attention on the resulting motions at the ends of a cell is obvious; it allows us to bypass the detailed motions of individual members

Wave Propagation Along Connected Identical Cells

Consider first the simplest case of wave propagation through identical cells that are connected end-to-end to form an array. Let these identical cells be labeled from left to right, m through n. In the absence of excitation, the state vectors at the two ends of the array are related, as follows:

where the arguments n_r and m_l for the transfer matrix $[T(n_r, m_l)]$ indicate the two ends of the array. Obviously, this transfer matrix may be computed from the transfer matrix of a single unit cell, as follows:

$$[T(n_r, m_l)] = [T(m_r, m_l)]^{n-m+1}$$
(13)

since all the cells in the array are identical. Converting the state vectors in Eq. (12) to wave vectors, we obtain the relationship

$$\begin{Bmatrix} \mu_r(n_r) \\ \mu_l(n_r) \end{Bmatrix} = [Q(n_r, m_l)] \begin{Bmatrix} \mu_r(m_l) \\ \mu_l(m_l) \end{Bmatrix}$$
(14)

where $[Q(n_r, m_l)]$ is a transfer matrix for wave vectors, and, in the present special case of identical cells, it is given by

$$[Q(n_r, m_l)] = [D(n)]^{-1} [T(n_r, m_l)][D(m)]$$

$$= \begin{bmatrix} \Lambda^{n-m+1} & 0 \\ 0 & \Lambda^{-(n-m+1)} \end{bmatrix}$$
 (15)

The second line of Eq. (15) is obtained by using Eq. (13) and recognizing the fact that [D(n)] = [D(m)]. The diagonal form of this wave vector transfer matrix indicates that the "resul-

$$\begin{array}{c|c}
 & n-1_r & n_l \\
\mu_r(n-1_r) & \longrightarrow & \longrightarrow \\
\mu_{\frac{1}{2}}(n-1_r) & \longrightarrow & \longrightarrow \\
\mu_{\frac{1}{2}}(n_{\frac{1}{2}}) & \longrightarrow & \mu_{\frac{1}{2}}(n_{\frac{1}{2}})
\end{array}$$

Fig. 3 Schematic of wave motions at the interface of two dissimilar cells.

tant" waves are transmitted through the entire array without reflection, although reduction of wave magnitudes can still occur due to damping.

Transmission and Reflection Matrices

Next consider the wave motions at the interface of two cells that are not identical. Let these two cells be numbered n-1 and n, as shown in Fig. 3. The relation between the wave vectors on the two sides of the interface may be written in the same form as Eq. (14), namely,

$$\begin{Bmatrix} \mu_r(n_l) \\ \mu_l(n_l) \end{Bmatrix} = \left[Q(n_b n - 1_r) \right] \begin{Bmatrix} \mu_r(n - 1_r) \\ \mu_l(n - 1_r) \end{Bmatrix}$$
(16)

where the transfer matrix for wave vector $[Q(n_b n - 1_r)]$ is now obtained as $[D(n)]^{-1}[D(n-1)]$, which is no longer a diagonal matrix.

It is illuminating to rearrange Eq. (16) in the form of an input-output relationship by viewing the incident waves $\mu_r(n-1_r)$ and $\mu_l(n_l)$ to the interface as inputs and outgoing waves $\mu_l(n-1_r)$ and $\mu_r(n_l)$ from the interface as outputs. Specifically, we write

$$\begin{Bmatrix} \mu_{l}(\mathbf{n} - \mathbf{1}_{r}) \\ \mu_{r}(\mathbf{n}_{l}) \end{Bmatrix} = \begin{bmatrix} R'(n_{b}n - 1_{r}) & T^{l}(n_{b}n - 1_{r}) \\ T'(n_{b}n - 1_{r}) & R^{l}(n_{b}n - 1_{r}) \end{bmatrix} \begin{Bmatrix} \mu_{r}(\mathbf{n} - \mathbf{1}_{r}) \\ \mu_{l}(\mathbf{n}_{l}) \end{Bmatrix}$$
(17)

The output $\mu_l(n-1_r)$ is seen to be the sum of the reflected portion of a right-going $\mu_r(n-1_r)$ and the transmitted portion of a left-going $\mu_l(n_l)$. Similarly, $\mu_r(n_l)$ is seen to be the sum of the transmitted portion of $\mu_l(n-1_r)$ and the reflected portion of $\mu_l(n_l)$. It is, therefore, logical to call submatrices T's in Eq. (17) the transmission matrices, and submatrices R's the reflection matrices. The arguments n_l and $n-1_r$ shown in the parentheses indicate that these matrices are associated with the interface between cells n and n-1, and the superscript r (or l) signifies that transmission or reflection is responding to a right-going (or a left-going) input wave vector.

Clearly, the transmission and reflection matrices can be computed from the wave transfer matrix [Q], and vice versa. By comparing Eqs. (16) and (17), it can be shown that

$$R'(j,i) = -[Q_{22}(j,i)]^{-1}Q_{21}(j,i)$$
 (18a)

$$T'(j,i) = Q_{11}(j,i) - Q_{12}(j,i)[Q_{22}(j,i)]^{-1}Q_{21}(j,i)$$
 (18b)

$$R^{I}(j,i) = Q_{12}(j,i)[Q_{22}(j,i)]^{-1}$$
 (18c)

$$T'(j,i) = [Q_{22}(j,i)]^{-1}$$
 (18d)

$$Q_{11}(j,i) = T^{r}(j,i) - R^{l}(j,i)[T^{l}(j,i)]^{-1}R^{r}(j,i)$$
(19a)

$$Q_{12}(j,i) = R^{l}(j,i)[T^{l}(j,i)]^{-1}$$
(19b)

$$Q_{21}(j,i) = -[T^l(j,i)]^{-1}R^r(j,i)$$
 (19c)

$$Q_{22}(j,i) = [T^{l}(j,i)]^{-1}$$
(19d)

where j > i.

Relations in Eqs. (18) and (19) are written in more general forms applicable to an arbitrary segment between two loca-

Free
$$\begin{vmatrix} F_L & m_L \\ --- & \mu_r(m_L) \\ --- & \mu_{L}(m_L) \end{vmatrix}$$

Fig. 4 A free boundary at the left end of cell m.

tions j and i along an array of cells, not necessarily on the two sides of an interface. It should be emphasized, however, that we have used a left-to-right numbering system, and the superscript r or l, referring to the right-going or a left-going input wave vector, must be interpreted accordingly.

In the special case of an array of identical cells, Eqs. (18) reduce to

$$R'(n_r, m_l) = R^l(n_r, m_l) = 0 (20a)$$

$$T^{r}(m_{r}, m_{l}) = T^{l}(n_{r}, m_{l}) = \Lambda^{n-m+1}$$
 (20b)

as expected.

Compositions of Transmission and Reflection Matrices

According to the chain rule for transfer matrices

$$Q(k,i) = Q(k,j)Q(j,i), \qquad i < j < k \tag{21}$$

four matrix equations can be obtained by expressing each transfer matrix in Eq. (21) in terms of the respective transmission and reflection matrices in the form of Eqs. (19). Solving the four matrix equations

$$R^r(k,i) = R^r(j,i)$$

$$+ T^{l}(j,i)R^{r}(k,j)[I - R^{l}(j,i)R^{r}(k,j)]^{-1}T^{r}(j,i)$$

$$T'(k,i) = T'(k,i)[I - R^{l}(j,i)R^{r}(k,i)]^{-1}T'(j,i)$$

$$R^{l}(k,i) = R^{l}(k,j)$$

$$+ T^{r}(k,j)R^{l}(j,i)[I - R^{r}(k,j)R^{l}(j,i)]^{-1}T^{l}(k,j)$$

$$T^{l}(k,i) = T^{l}(j,i)[I - R^{r}(k,j)R^{l}(j,i)]^{-1}T^{l}(k,j), \quad i < j < k \quad (22)$$

These are the rules by which the transmission and reflection matrices for two connected segments can be computed from those of individual segments.

Reflection at a Boundary

Two types of boundary conditions will be considered. The clamped boundary condition requires that displacements be zero, and the free boundary condition requires that forces be zero. All waves must be totally reflected at either type of boundary, which means that elements of the transmission matrices characterizing a boundary must be all zeros. The reflection matrices, however, depend on whether the boundary conditions are clamped or free.

As shown in Fig. 4, let cell m be an end cell next to a left-hand-side boundary. The state and wave vectors are related, as follows:

$$\begin{Bmatrix} w(m_l) \\ f(m_l) \end{Bmatrix} = \begin{bmatrix} M_r(m) & M_l(m) \\ N_r(m) & N_l(m) \end{bmatrix} \begin{Bmatrix} \mu_r(m_l) \\ \mu_l(m_l) \end{Bmatrix}$$
(23)

If m_l is next to a free boundary, then $f(m_l) = 0$. From the second row of Eq. (23), we obtain

$$\mu_r(m_l) = -[N_r(m)]^{-1}N_l(m)\mu_l(m_l) \tag{24}$$

At the boundary, $\mu_l(m_l)$ may be treated as the input and $\mu_r(m_l)$ treated as the output. Thus, we also have

$$\mu_r(m_l) = R^l(m_b F_l) \mu_l(m_l) \tag{25}$$

where $R^{\prime}(m_{l},F_{l})$ is the reflection matrix of a left-hand-side free boundary associated with a left-going incident wave vector. Comparing Eqs. (24) and (25),

$$R'(m_l, F_l) = -[N_r(m)]^{-1} N_l(m)$$
 (26a)

In addition, the transmission matrix of a left-hand-side free boundary must be

$$T^{l}(m_{l},F_{l})=0 \tag{26b}$$

Other cases can be similarly treated.³ If m_l is next to a clamped boundary, then

$$R^{l}(m_{b}C_{l}) = -[M_{r}(m)]^{-1}M_{l}(m)$$
 (27a)

$$T^{l}(m_{l},C_{l})=0 (27b)$$

If cell *m* is an end cell next to a right-hand-side free boundary, then

$$R'(F_r, m_r) = -[N_l(m)]^{-1}N_r(m)$$
 (28a)

$$T'(F_r, m_r) = 0 (28b)$$

If cell m is an end cell next to a right-hand-side clamped boundary, then

$$R'(C_r, m_r) = -[M_l(m)]^{-1}M_r(m)$$
 (29a)

$$T^r(C_r, m_r) = 0 (29b)$$

For mixed boundary conditions, namely, when only certain displacement components and certain force components must vanish at the boundary, it will be necessary to rearrange the state vector $\{w, f\}$, such that the vanishing components are grouped in either the upper half or the lower half of the new state vector. The rows in the M and N matrices in Eq. (23) must also be rearranged correspondingly, and the reflection and transmission matrices can then be obtained in a similar manner.

Input-out Relationship for One-dimensional Cell-array

A one-dimensional cell-array is shown in Fig. 5. Such an array may be composed of several sections of periodic structures, and different sections may be composed of different cell units. By use of the composition rules [Eqs. (22)], the transmission and reflection matrices can be determined for any segment of the array between two arbitrary locations in the array.

To show how the response of the structure to an excitation can be obtained in the frequency domain for this structure, let us assume that both ends of the cell-array are free, and that an input is applied at the interface between S_r and $S+1_l$. Our objective is to calculate the responses at j_r and k_l , where $1 \le j \le S$ and $S+1 \le k \le N$.

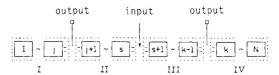


Fig. 5 A chain of connected cells with excitations applied at the interface between cell S and cell S+1.

The input causes a discontinuity between the state vectors at S_r and $S + 1_l$. This is expressed in an equation

$$\begin{Bmatrix} w_S \\ f_S \end{Bmatrix} = \begin{Bmatrix} w(S+1_l) \\ f(S+1_l) \end{Bmatrix} - \begin{Bmatrix} w(S_r) \\ f(S_r) \end{Bmatrix}$$
(30)

Transforming the state vectors, $\{w(S+1_l), f(S+1_l)\}\$ and $\{w(S_r), f(S_r)\}\$, into wave vectors, we obtain

$$\begin{cases} w_S \\ f_S \end{cases} = \begin{bmatrix} M_r(S+1) & M_l(S+1) \\ N_r(S+1) & N_l(S+1) \end{bmatrix} \begin{cases} \mu_r(S+1_l) \\ R'(F_r,S+1_l)\mu_r(S+1_l) \end{cases}$$

$$-\begin{bmatrix} M_r(S) & M_l(S) \\ N_r(S) & N_l(S) \end{bmatrix} \begin{Bmatrix} R^l(S_r, F_l)\mu_l(S_r) \\ \mu_l(S_r) \end{Bmatrix}$$
(31)

In the above equation, we have replaced $\mu_l(S + \mathbf{1}_l)$ by $R'(F_r, S + \mathbf{1}_l)\mu_r(S + \mathbf{1}_l)$ and $\mu_r(S_r)$ by $R^l(S_r, F_l)\mu_l(S_r)$. Rearranging,

$$\begin{pmatrix} \mu_r(S+1_l) \\ \mu_l(S_r) \end{pmatrix} = \begin{bmatrix} M_r(S+1) + M_l(S+1)R^r(F_r,S+1_l) \\ N_r(S+1) + N_l(S+1)R^r(F_r,S+1_l) \end{bmatrix}$$

$$-M_{r}(S)R^{l}(S_{r}F_{l}) - M_{l}(S) - N_{r}(S)R^{l}(S_{r}F_{l}) - N_{l}(S) - N_{r}(S)R^{l}(S_{r}F_{l}) - N_{l}(S)$$
(32)

This equation shows how a right-going wave vector $\mu_r(S+1_l)$ and a left-going wave vector $\mu_l(S_r)$ are generated by the inputs w_S and f_S , and how the structural constructions on the two sides of the inputs, as well as the boundary conditions, affect the wave generation. Usually, inputs to a physical system are forces, in which case $w_s=0$. However, Eq. (32) also shows that "displacement inputs" which cause discontinuities in the displacements, can also be considered. Moreover, the natural frequencies of the system can be obtained from Eq. (32). At a natural frequency, the matrix inversion indicated on the right-hand-side of this equation does not exist, or the determinant of the original matrix vanishes. Of course, when computing the natural frequencies, the system is undamped.

The responses at locations j_r and k_l can be obtained quite simply, as follows:

$$\begin{cases}
w(j_r) \\
f(j_r)
\end{cases} = [D(j)] \begin{cases} \mu_r(j_r) \\ \mu_l(j_r) \end{cases} \\
= \begin{bmatrix} M_r(j) & M_l(j) \\ N_r(j) & N_l(j) \end{bmatrix} [Q(j_r, S_r)] \begin{cases} R^l(S_r, F_l) \mu_l(S_r) \\ \mu_l(S_r) \end{cases}, \quad j \leq S$$
(33)

$$\begin{cases}
w(k_l) \\
f(k_l)
\end{cases} = [D(k)] \begin{Bmatrix} \mu_r(k_l) \\
\mu_l(k_l)
\end{Bmatrix}$$

$$= \begin{bmatrix} M_r(k) & M_l(k) \\
N_r(k) & N_l(k)
\end{bmatrix} [Q(k_b S + 1_l)]$$

$$\times \begin{Bmatrix} \mu_r(S + 1_l) \\
R'(F_r S + 1_l) \mu_r(S + 1_l)
\end{Bmatrix}, \quad k \ge S + 1 \tag{34}$$

The wave transfer matrices Q's in the above equations may be expressed in terms of the reflection and transmission matrices, if desired. Then the displacement responses, for example, are given by

$$w(j_r) = [M_r(j)R^l(j_r, F_l) + M_l(j)][I - R^r(S_r, j_r)R^l(j_r, F_l)]$$

$$-1T^l(S_r, j_r)\mu_l(S_r), \qquad j \le S$$

$$w(k_l) = [M_r(k) + M_l(k)R^r(F_r, k_l)]$$

$$\times [I - R^l(k_l, S_l + 1_l)R^r(F_r, k_l)]^{-1}$$
(35)

$$\times T'(k_b S + 1_l)\mu_r(S + 1_l), \qquad k \ge S + 1$$
 (36)

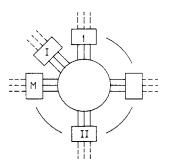


Fig. 6 An M + 2-array intersection.

The force responses can be obtained simply by replacing M by N in Eqs. (35) and (36). If one or both boundaries are clamped, the solution may be modified by replacing F by C, as required. The solutions are also valid at the boundaries, in which case $j_r = 1_l$ and $k_l = N_r$.

Intersecting Cell-arrays

In the foregoing, truss cells are assumed to be connected end-to-end to form an array. The resulting structure is essentially one dimensional in space, for which the transfer matrix formulation is most convenient for the analysis. The case of intersecting arrays is a variation of this basic configuration; therefore, some modification is required for its analysis.

Figure 6 shows M + 2 intersecting cell-arrays that share a common core-cell. Each array is constructed of one-dimensional piece-wise periodic cells. We label these arrays by the numbers I, II, 1, 2, ..., M, the first two being Roman numerals. Each of these numbers will also be used to indicate the interface between the core-cell and an array (dashed lines in the figure) for the purpose of identifying the displacements and/or forces at that interface. Since the superposition principle holds for a linear structure, no generality is lost by assuming that only one excitation vector is present and is located at the core-cell, or on either array I or array II. The strategy we shall adopt in our analysis is to modify the core-cell by lumping on it the effect of unloaded arrays 1 through M. By so doing, the modified core-cell and the connected arrays I and II may be treated as an equivalent one-dimensional array. Thus, the subsequent analysis may proceed in the same manner as that of the one-dimensional array given in the previous section. Any boundary conditions at the far end of an unloaded array 1 through M can be treated. For illustration purposes, however, all these ends will be assumed to be free. The choice of arrays I and II is quite arbitrary. Of course, the resulting equivalent one-dimensional structure, consisting sequentially of array I, the modified core-cell, and array II must contain both the input and output stations.

We shall consider a more general case in which an excitation vector f_{ext} is located on the core-cell. The components of this excitation vector may consist of several forces acting at a number of node points, which will be referred to as inner coordinates. Displacements at all the inner coordinates will be denoted by vector w_{inn} . The interfaces between the core-cell and cell-arrays will be referred to as outer coordinates. Displacements and forces at all the outer coordinates will be denoted by w and f_{r} respectively.

Using a finite-element method, the dynamical equation for the core-cell shown in Fig. 6 may be expressed as follows:

$$\begin{bmatrix} P_{11} & P_{12} \\ P_{21} & P_{22} \end{bmatrix} \begin{Bmatrix} w \\ w_{inn} \end{Bmatrix} = \begin{Bmatrix} f \\ f_{ext} \end{Bmatrix}$$
(37)

where P_{ij} are subimpedance matrices. Eliminating w_{inn} from the above equation yields

$$[P_{11} - P_{12} P_{22}^{-1} P_{21}] \{ w \} = \{ f \} - P_{12} P_{22}^{-1} \{ f_{ext} \}$$
 (38)

To proceed further, rewrite Eq. (38) in the following form:

$$[A] \begin{cases} w(I) \\ w(II) \\ w(I) \\ \vdots \\ w(M) \end{cases} = \begin{cases} f(I) \\ f(II) \\ f(I) \\ \vdots \\ f(M) \end{cases} + \begin{cases} F_1 \\ F_{II} \\ F_1 \\ \vdots \\ F_M \end{cases}$$
(39)

in which

$$[A] = P_{11} - P_{12} P_{22}^{-1} P_{21}$$
 (40)

and

$$\begin{cases}
F_{1} \\
F_{11} \\
F_{1} \\
\vdots \\
F_{M}
\end{cases} = -P_{12} P_{22}^{-1} \{f_{ext}\} \tag{41}$$

Transforming the state vector at the outer coordinate j of the core-cell into wave vectors, we have

$$\begin{Bmatrix} w(j) \\ f(j) \end{Bmatrix} = \begin{bmatrix} M_o(j) & M_i(j) \\ N_o(j) & N_i(j) \end{bmatrix} \begin{Bmatrix} \mu_o(j) \\ \mu_i(j) \end{Bmatrix}$$
(42)

where subscript i or o associated with a wave vector signifies an incoming or an outgoing wave when referring to the corecell. Equation (39) then can be written as

$$[B] \begin{cases} \mu_o(I) \\ \vdots \\ \mu_o(M) \\ \mu_i(I) \\ \vdots \\ \mu_i(M) \end{cases} = \begin{cases} F_1 \\ \vdots \\ F_M \end{cases}$$

$$(43)$$

where

$$-\begin{bmatrix} N_{o}(I) & & N_{i}(I) & & & & & \\ & \cdot & & 0 & & \cdot & & 0 \\ & & \cdot & & & & \cdot & & \\ 0 & & \cdot & & 0 & & \cdot & \\ & & & N_{o}(M) & & & N_{i}(M) \end{bmatrix}$$
(44)

Note that the number of columns is two times the number of rows in matrix B. By separating B into two square matrices, namely, $B = [B_1, B_2]$, Eq. (43) can be recast into the following form:

$$\begin{cases}
\mu_{o}(I) \\
\mu_{o}(II) \\
\mu_{o}(I) \\
\vdots \\
\mu_{o}(M)
\end{cases} = [S] \begin{cases}
\mu_{i}(I) \\
\mu_{i}(II) \\
\mu_{i}(I) \\
\vdots \\
\mu_{i}(M)
\end{cases} + [G] \begin{cases}
F_{I} \\
F_{II} \\
F_{I} \\
\vdots \\
F_{M}
\end{cases} (45)$$

where $S = -B_1^{-1}$ B_2 and $G = B_1^{-1}$. Matrices S and G are called the wave scattering matrix and the wave-mode genera-

tion matrix, respectively.⁴ The former redirects the incoming waves to outgoing directions, and the latter converts the external forces into wave sources, namely,

$$\begin{cases}
\mu_{s}(I) \\
\mu_{s}(II) \\
\mu_{s}(1) \\
\vdots \\
\mu_{s}(M)
\end{cases} = [G] \begin{cases}
F_{1} \\
F_{11} \\
F_{1} \\
\vdots \\
F_{M}
\end{cases}$$
(46)

The resulting out-going waves are, of course, the sum of the above two types of contributions.

The scattering matrix S is composed of $(M + 2) \times (M + 2)$ submatrices S_{kj} ; k, j = I, II, 1, ..., M. Each S_{kj} is a transmission matrix, if $j \neq k$. It redirects an incoming wave $\mu_i(j)$ to the kth direction, and it becomes a reflection matrix, if j = k. The important properties of scattering matrices are discussed, for example, in Ref. 15.

Note that when referring to the entire array j, $\mu_o(j)$ becomes an incoming wave and $\mu_i(j)$ becomes an outgoing wave. Since array j is unloaded, $\mu_i(j)$ can also be considered as a reflected wave from the far-end boundary. It follows from Eq. (45) that

$$\begin{pmatrix}
\mu_o(I) \\
\mu_o(II) \\
\mu_o(1) \\
\vdots \\
\mu_o(M)
\end{pmatrix} = [S] \begin{bmatrix}
I \\
I & 0 \\
R^o(1) \\
0 & R^o(M)
\end{bmatrix}$$

$$\times \begin{cases}
\mu_{i}(\mathbf{I}) \\
\mu_{i}(\mathbf{I}) \\
\mu_{o}(\mathbf{1}) \\
\vdots \\
\mu_{o}(M)
\end{cases} + \begin{cases}
\mu_{s}(\mathbf{I}) \\
\mu_{s}(\mathbf{I}) \\
\vdots \\
\mu_{s}(M)
\end{cases} \tag{47}$$

where each $R^{o}(j)$, j = 1, 2, ..., M, is a reflection matrix associated with the far-end boundary of array j. Equation (47) can be simplified to

$$\begin{pmatrix}
\mu_{o}(\mathbf{I}) \\
\mu_{o}(\mathbf{II}) \\
0 \\
\vdots \\
0
\end{pmatrix} = \begin{bmatrix}
U_{11} & U_{12} \\
U_{21} & \overline{U}_{22}
\end{bmatrix} \begin{pmatrix}
\mu_{i}(\mathbf{I}) \\
\mu_{i}(\mathbf{II}) \\
\mu_{o}(\mathbf{1}) \\
\vdots \\
\mu_{o}(M)
\end{pmatrix} + \begin{pmatrix}
\mu_{s}(\mathbf{I}) \\
\mu_{s}(\mathbf{II}) \\
\mu_{s}(\mathbf{I}) \\
\vdots \\
\mu_{s}(M)
\end{pmatrix} (48)$$

in which U_{ij} are submatrices of

$$U = [S] \begin{bmatrix} I & 0 & \cdot & \cdot & \cdot & 0 \\ 0 & I & & \cdot & \cdot \\ \cdot & R^{o}(1) & & \vdots \\ \vdots & & \cdot & \cdot & 0 \\ 0 & \cdot & \cdot & \cdot & 0 & R^{o}(M) \end{bmatrix}$$
(49)

and $\overline{U}_{22} = U_{22} - [I]$.

The wave vectors $\mu_o(1)$ through $\mu_o(M)$ can be eliminated from Eq. (48) using the lower rows of the equation, resulting in

$$\begin{Bmatrix} \mu_{o}(\mathbf{I}) \\ \mu_{o}(\mathbf{II}) \end{Bmatrix} = \left[U_{11} - U_{12}\overline{U}_{22}^{-1}U_{21} \right] \begin{Bmatrix} \mu_{i}(\mathbf{I}) \\ \mu_{i}(\mathbf{II}) \end{Bmatrix} + \begin{Bmatrix} \mu_{s}(\mathbf{I}) \\ \mu_{s}(\mathbf{II}) \end{Bmatrix}$$

$$- U_{12}\overline{U}_{22}^{-1} \begin{Bmatrix} \mu_{s}(1) \\ \vdots \\ \mu_{s}(M) \end{Bmatrix}$$
(50)

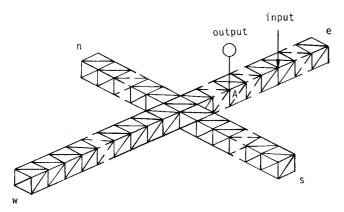


Fig. 7 Schematic of an example space structure.

Equation (50) is a relationship among the incoming waves, the outgoing waves, and the source waves, with the effects of unloaded arrays 1 through M taken fully into account. The source waves are generated by the external forces at the inner coordinates of the core-cell (represented by solid lines in Fig. 6). The form of Eq. (50) clearly suggests that the entire structure has been replaced by an equivalent one-dimensional array. Thus, results obtained in the previous sections can be applied to the present case.

Let array I be treated as being on the left of array II, and let Eq. (50) be recast in an alternate form, as follows:

$$\begin{Bmatrix} \mu_{l}(\mathbf{I}) \\ \mu_{r}(\mathbf{II}) \end{Bmatrix} = \left[U_{11} - U_{12} \overline{U}_{22}^{-1} U_{21} \right] \begin{Bmatrix} \mu_{r}(\mathbf{I}) \\ \mu_{l}(\mathbf{II}) \end{Bmatrix} + \begin{Bmatrix} \mu_{s}(\mathbf{I}) \\ \mu_{s}(\mathbf{II}) \end{Bmatrix}$$

$$- U_{12} \overline{U}_{22}^{-1} \begin{Bmatrix} \mu_{s}(1) \\ \vdots \\ \mu_{s}(M) \end{Bmatrix} \tag{51}$$

The square matrix on the right-hand-side in the above equation is clearly a scattering matrix; thus, it can be identified as

$$[U_{11} - U_{12}\overline{U}_{22}^{-1}U_{21}] = \begin{bmatrix} R'(II,I) & T'(II,I) \\ T'(II,I) & R'(II,I) \end{bmatrix}$$
(52)

and it includes the effects of unloaded arrays 1 through M.

Recall that we consider only one external excitation vector located on the core-cell. Since arrays I and II are unloaded, $\mu_r(\mathbf{I})$ and $\mu_I(\mathbf{II})$ can be expressed in terms of $\mu_l(\mathbf{I})$ and $\mu_r(\mathbf{II})$, namely,

$$\begin{Bmatrix} \mu_r(\mathbf{I}) \\ \mu_l(\mathbf{II}) \end{Bmatrix} = \begin{bmatrix} R^l(\mathbf{I}, F_l) & 0 \\ 0 & R^r(F_l, \mathbf{II}) \end{bmatrix} \begin{Bmatrix} \mu_l(\mathbf{I}) \\ \mu_r(\mathbf{II}) \end{Bmatrix}$$
(53)

Then Eq. (51) can be rewritten as

$$\begin{Bmatrix} \mu_{I}(\mathbf{I}) \\ \mu_{r}(\mathbf{II}) \end{Bmatrix} = [L]^{-1} \begin{Bmatrix} \mu_{s}(\mathbf{I}) \\ \mu_{s}(\mathbf{II}) \end{Bmatrix} - U_{12} \overline{U}_{22}^{-1} \begin{Bmatrix} \mu_{s}(\mathbf{I}) \\ \vdots \\ \mu_{s}(M) \end{Bmatrix}$$
(54)

where

$$[L] = [I] - [U_{11} - U_{12}\overline{U}_{22}^{-1}U_{21}] \begin{bmatrix} R^{i}(I, F_{l}) & 0\\ 0 & R^{r}(F_{l}, II) \end{bmatrix}$$
 (55)

and where use has been made of the free boundary conditions at the far ends of arrays I and II. The response at any location on these two arrays can easily be obtained by substituting Eq. (54) into Eqs. (35) and (36), noting that the interface I corresponds to S_r and the interface II corresponds to S_r and S_r

On the other hand, if external excitations are not located on the core-cell, but on either array I or II, then the source waves $\mu_s(I)$, $\mu_s(II)$, $\mu_s(1)$, ..., $\mu_s(M)$ disappear from Eq. (51). In this case, the net effect of the core-cell and the unloaded arrays 1 through M is represented only by the reflection and transmission matrices given in Eq. (52).

Numerical Example

A schematic of a space structure is shown in Fig. 7. This structure consists of two intersecting arrays of truss-cell units, with 81 periodic units in the *w-e* direction and 61 periodic units in the *n-s* direction. The ends of both arrays are free. The core-cell at the intersection is the 31st, counting from the south end, and is the 21st, counting from the west end. Each truss cell is composed of eighteen bars. The diagonal bars are $\sqrt{2}$ m long; nondiagonal bars are 1 m long. All bars have the same cross-sectional area 5.03×10^{-3} m². The cross section has the same moments of inertia 2.01×10^{-6} m⁴ about the two principal axes, and the same polar moment of inertia 4.02×10^{-6} m⁴. In the calculation, we use a complex Young's modulus $E = 69.6 \times 10^9$ (1 + $i\gamma$ sgn ω) Newton per m² with a loss factor $\gamma = 0.04$, mass density $\rho = 3.77 \times 10^3$ kg/m³, and Poisson ratio $\nu = 0.32$.

The input is a concentrated moment about a *w-e* axis (interpreted according to the right-hand rule) and applied at the interface between the 21st and the 22nd cells, counting from the east end. Wave scatterings are expected at the intersection and the four boundaries. The output is calculated at the interface between the 35th and 36th cells from the east end.

The computed amplitude of the frequency response for the angle of rotation at point A about an s-n axis is shown in Fig. 8. Significant response can be seen between 800 and 2500 rad/s. This frequency interval appears to coincide with the

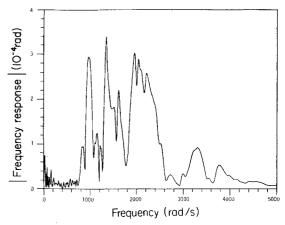


Fig. 8 Amplitude of frequency response of rotational angle about an s-n axis at point A.

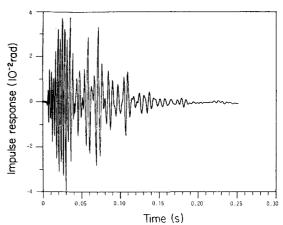


Fig. 9 Impulse response of rotational angle about an s-n axis at point A.

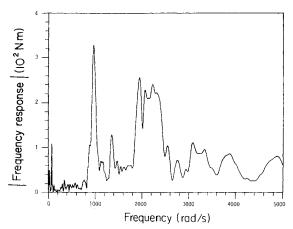


Fig. 10 Amplitude of frequency response of moment about a vertical axis at point A.

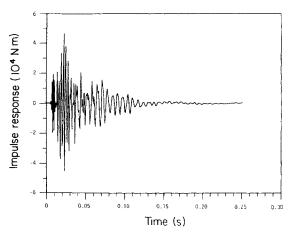


Fig. 11 Impulse response of moment about a vertical axis at point A.

first two wave-passage frequency bands^{3,8,16,17} for an ideal periodic truss structure. Responses in higher bands are considerably lower. The use of a lower loss factor γ will increase the response in the higher bands, but it will not cause any numerical difficulties.

The impulse response obtained from applying the fast Fourier transform (FFT) to the frequency response is shown in Fig. 9, using a frequency step of 10 rad/s. By computing the phase velocities of various waves, their contributions in this time-domain plot can also be identified.³ The waves from the second band begin to arrive at 0.005 s after an impulsive excitation, whereas the waves from the first band begin to arrive at 0.04 s. These account for two major bursts, shown in Fig. 9. Signals appearing after 0.1 s are attributable to reflected waves from the boundaries and the intersection. Since all cells are identical in this particular structure, the FFT program can also be applied to individual wave modes separately, and the results are summed to obtain the total response. However, such an alternative procedure is found to be of little advantage, and it is, in fact, more cumbersome when the structure is composed of several types of cells.

Figures 10 and 11 show the amplitude of frequency response and impulse response, respectively, for the moment at A about a vertical axis. Comments similar to those related to Figs. 8 and 9 can also be made for these figures.

Concluding Remarks

The numerical procedure presented herein is both efficient and accurate for the analysis of truss-type space structures composed of spatially periodic truss units or piece-wise periodic units. Typical truss units are modeled using a finite-element approach to achieve whatever modeling accuracy required. Traditional transfer matrices for state vectors are transformed to transfer matrices for wave vectors, so that various wave motions propagating along the structure in two opposite directions can be identified. Except for approximations that may be inherent in the finite-element modeling, the analysis is exact.

The unique feature of the procedure is the employment of transmission and reflection matrices in order that computation always proceeds in the direction of wave propagation, and the numerical difficulty associated with the traditional transfer matrix approach can be circumvented when the structure is long or when a large number of wave motions is involved. The use of transmission and reflection matrices also facilitates the treatment of such complicated configurations as intersecting cell-arrays.

Although our general scheme follows that of von Flotow,⁴ the technical developments presented herein are quite independent and different in many details. Our main emphasis is placed on the response of *real* structures to external excitations where structural damping is always present. The response, rather than other characteristics (see, e.g., Ref. 14), is believed to be more important to design engineers. We have provided specific formulas required for step-by-step computation involving complicated structural cells and specific boundary conditions. When the theory is applied to example problems, we did not encounter numerical difficulties of the type described in Ref. 4.

Acknowledgment

This paper is prepared under grant AFOSR-88-005 from the Air Force Office of Scientific Research, Air Force Systems Command, USAF, monitored by Anthony Amos. The U.S. Government is authorized to reproduce and distribute reprints for governmental purposes, notwithstanding any copyright notation thereon.

References

¹Noor, A. K., and Anderson, M. S., "Continuum Model for Beamand Plate-Like Lattice Structures," *AIAA Journal*, Vol. 16, Dec. 1978, pp. 1219–1228.

²Sun, C. T., Kim, B. J., and Bogdanoff, "On the Derivation of Equivalent Simple Models for Beam- and Plate-Like Structures in Dynamic Analysis," *Proceedings of the 1981 AIAA Dynamics Specialists Conference*. April 1981, pp. 523-532.

cialists Conference, April 1981, pp. 523-532.

³Yong, Y., and Lin, Y. K., "Propagation of Decaying Waves in Periodic and Piece-Wise Periodic Structures," Journal of Sound and Vibration, Vol. 129, No. 2, 1989, pp. 99-118.

⁴von Flotow, A. H., "Disturbance Propagation in Structural Network," *Journal of Sound and Vibration*, Vol. 106, No. 3, 1986, pp. 433-450.

⁵Lin, Y. K., and McDaniel, T. J., "Dynamics of Beam-Type Periodic Structures," *Journal of Engineering for Industry*, Vol. 91, Nov. 1969, pp. 1133–1141.

⁶Lin, Y. K., and Donaldson, B. K., "A Brief Survey of Transfer Matrix Techniques with Special Reference to the Analysis of Aircraft Panels," *Journal of Sound and Vibration*, Vol. 10, No. 1, 1969, pp. 103-143.

⁷Lin, Y. K., "Random Vibration of Periodic and Almost Periodic Structures," *Mechanics Today*, edited by S. Nemat-Nasser, Pergamon Press, New York, 1976, pp. 93-124.

⁸Mead, D. J., "Free Wave Propagation in Periodically Supported Infinite Beams," *Journal of Sound and Vibration*, Vol. 11, No. 2, 1970, pp. 181-197.

⁹Mead, D. J., and Sen Gupta, G., "Natural Flexural Waves and Normal Modes of Periodically Supported Beams and Plates," *Journal of Sound and Vibration*, Vol. 13, No. 1, 1970, pp. 89-101.

¹⁰Mead, D. J., "A General Theory of Harmonic Wave Propagation in Linear Periodic Systems with Multiple Coupling," *Journal of*

Sound and Vibration, Vol. 27, No. 2, 1973, pp. 235-260.

¹¹Mead, D. J., "Wave Propagation and Natural Modes in Periodic Systems: I. Mono-Coupled Systems, II. Multi-Coupled Systems, With and Without Damping," Journal of Sound and Vibration, Vol. 40, No. 1, 1975, pp. 1-39.

¹²Mead, D. J., and Markus, S., "Coupled Flexural-Longitudinal Wave Motion in Periodic Beams," Journal of Sound and Vibration, Vol. 90, No. 1, 1983, pp. 1-24.

¹³McDaniel, T. J., and Eversole, K. B., "A Combined Finite-Element-Transfer Matrix Structural Analysis Method," Journal of Sound and Vibration, Vol. 51, No. 2, 1977, pp. 157-169.

¹⁴Signorell, J., and von Flotow, A. H., "Wave Propagation, Power Flow, and Resonance in a Truss Beam," Journal of Sound and Vibration, Vol. 126, No. 1, 1988, pp. 127-144.

¹⁵Helszajn, J., Nonreciprocal Microwave Junctions and Circulators, Wiley, New York, 1975.

¹⁶Brillouin, Wave Propagation in Periodic Structures, Dover, New

¹⁷Miles, J. W., "Vibrations of Beams on Many Supports," Engineering Mechanics Division, ASCE 82, EM1, 1953, pp. 1-9.

Recommended Reading from the AIAA Progress in Astronautics and Aeronautics Series



Dynamics of Explosions and Dynamics of Reactive Systems, I and II

J. R. Bowen, J. C. Lever, and R. I. Soloukhin, editors

Companion volumes, Dynamics of Explosions and Dynamics of Reactive Systems, I and II, cover new findings in the gasdynamics of flows associated with exothermic processing—the essential feature of detonation waves—and other, associated phenomena.

Dynamics of Explosions (volume 106) primarily concerns the interrelationship between the rate processes of energy deposition in a compressible medium and the concurrent nonsteady flow as it typically occurs in explosion phenomena. Dynamics of Reactive Systems (Volume 105, parts I and II) spans a broader area, encompassing the processes coupling the dynamics of fluid flow and molecular transformations in reactive media, occurring in any combustion system. The two volumes, in addition to embracing the usual topics of explosions, detonations, shock phenomena, and reactive flow, treat gasdynamic aspects of nonsteady flow in combustion, and the effects of turbulence and diagnostic techniques used to study combustion phenomena.

Dynamics of Explosions 1986 664 pp. illus., Hardback ISBN 0-930403-15-0 AIAA Members \$49.95 Nonmembers \$84.95 Order Number V-106

Dynamics of Reactive Systems I and II 1986 900 pp. (2 vols.), illus. Hardback ISBN 0-930403-14-2 AIAA Members \$79.95 Nonmembers \$125.00 Order Number V-105

TO ORDER: Write, Phone, or FAX: AIAA c/o TASCO, 9 Jay Gould Ct., P.O. Box 753, Waldorf, MD 20604 Phone (301) 645-5643, Dept. 415 = FAX (301) 843-0159

Sales Tax: CA residents, 7%; DC, 6%. Add \$4.75 for shipping and handling of 1 to 4 books (Call for rates on higher quantities). Orders under \$50.00 must be prepaid. Foreign orders must be prepaid. Please allow 4 weeks for delivery. Prices are subject to change without notice. Returns will be accepted within 15 days.